Available online at www.sciencedirect.com
ScienceDirect
Trans. Nonferrous Met. Soc. China 33(2023) 902−916
Transactions of Nonferrous Metals Society of China
www.tnmsc.cn

# Improving vanadium extraction from refractory stone coal by suspension roasting

Shuai YUAN[1,2], Yong-hong QIN[1,2], Yong-peng JIN[1,2], Yan-jun LI[1,2]

1. College of Resources and Civil Engineering, Northeastern University, Shenyang 110819, China;
2. National-local Joint Engineering Research Center of High-efficient Exploitation Technology for Refractory Iron Ore Resources, Shenyang 110819, China

Received 24 December 2021; accepted 17 May 2022

**Abstract:** An innovative suspension roasting−leaching technology in the atmosphere was proposed to improve the vanadium extraction from refractory stone coal. The leaching rate of vanadium was enhanced from 20% previously to 47.14% by present technology at a roasting temperature of 800 °C, a roasting time of 20 min, and a gas flow rate of 400 mL/min. Throughout the suspension roasting process, the surface of the stone coal gradually became rough and irregular. The specific surface area of the particles increased and the lamellar structure of the silicate minerals was destroyed, contributing to the release of vanadium. Meanwhile, the vanadium in the stone coal was oxidized to V(V) or V(IV). The results indicated that the leaching rate was improved owing to the release and transformation of vanadium in the suspension roasting.

**Key words:** stone coal; vanadium; suspension roasting; leaching; phase reconstruction; microstructure

## 1 Introduction

Vanadium, a rare metal with strategic significance, is mainly used in the iron and steel industry, aerospace, chemical industry, and energy storage field [1−5]. Vanadium is widely distributed in vanadium titanomagnetite, green sulfur vanadium ore, vanadium potassium uranium ore, vanadium calcium copper ore, vanadium-bearing mica, asphalt minerals, coal, and oil shale [2]. However, due to its earth abundance and multiple stable oxidation states, vanadium can form compounds with various elements that are dispersed during the mineralization process. As a result, even the vanadium ores of industrial value rarely reach grades above 1% currently. So far, the global vanadium reserves have been $2\times10^7$ t (vanadium content), of which China's vanadium reserves are $9.5\times10^6$ t, accounting for 47.5% of the world's total reserves [2]. Stone coal is a unique vanadium resource in China, with vanadium content generally ranging from 0.3 wt.% to 1.2 wt.% [2,6].

According to statistics, vanadium-bearing stone coal reserves are enormous [7,8]. The form of vanadium in the ore directly affects the method and ease of vanadium extraction. So far, multiple extraction processes of vanadium from stone coal have been developed, including traditional gravity separation [9,10], flotation [11−13], direct leaching [2], heating and pressure leaching [14], acid curing−water leaching [2], microwave pretreatment−leaching [2], sodium roasting−water leaching [15], calcification roasting−water leaching [16,17], and oxidation roasting−leaching [18,19]. In China, most of the vanadium in stone coal exists in the mica (silicate minerals) crystal lattice in the form of isomorphism, and it is not easy to achieve high-quality recycling of vanadium through a single conventional beneficiation technology [20−22]. For

**Corresponding author:** Yong-hong QIN, E-mail: qyh_neu@163.com
DOI: 10.1016/S1003-6326(23)66154-0

vanadium extraction, the crystal structure of the silicate minerals should be destroyed to release the vanadium present in the crystal structure. Nevertheless, silicate minerals are structurally stable, whereby high-temperature roasting is usually used to disrupt the mineral lattice while oxidizing V(III) to V(IV) or V(V) for subsequent leaching treatment.

Nonetheless, the traditional roasting−leaching process has several drawbacks, such as serious environmental pollution, low stone coal conversion, low recovery, slow reaction rate, susceptibility to sintering, poor product uniformity, and high acid consumption, rendering it difficult to be applied to a large scale [2,9−19,23,24]. The suspension roasting technology proposed by the Northeastern University of China has been widely used to exploit various complex and difficult mineral resources with excellent results [25−29]. Based on the basic principle of fluidization technology, the ore is suspended under the action of gas flow, and the contact between the hot gas flow and the ore particles is fully utilized to accelerate the roasting reaction. For this work, typical refractory stone coal was selected, subjected to a traditional roasting−leaching process, leaving a vanadium leaching rate of only approximately 20%. Given the high productivity, fast reaction rate, and low energy consumption of suspension roasting, an innovative suspension roasting−acid leaching technique was proposed to extract vanadium from stone coal efficiently.

In this study, suspension roasting experiments were conducted on vanadium-bearing stone coal. The effects of roasting temperature, roasting time, and gas flow rate on vanadium extraction were investigated according to the content of carbon and the leaching rate. The phase transformation, structural variation, surface morphology, and pore distribution characteristics were analyzed to discuss the mechanism of vanadium extraction enhanced by suspension roasting. Besides, phase reconstruction and vanadium transformation behavior during suspension roasting were discussed.

## 2 Experimental

### 2.1 Materials

The raw ore was collected from Dunhuang, Gansu Province, China. The ore sample was crushed to ≤0.5 mm by a jaw crusher and a counter roller crusher. The results of the chemical composition analysis of raw ore were shown in Table 1. From Table 1, the main valuable element in the ore was V, with the $V_2O_5$ content of 0.98 wt.%. $SiO_2$ (63.7 wt.%) and $Al_2O_3$ (10.46 wt.%) were the main gangue components. In addition, the contents of CaO, $K_2O$, and MgO were 3.45 wt.%, 2.19 wt.%, and 1.19 wt.%, respectively. The carbon content was 14.15 wt.%. Since the vanadium was wrapped by carbon and the leaching agent was consumed to increase the difficulty of vanadium extraction, it was imperative to decarbonize the ore by roasting. The results of the coal industry analysis of the vanadium-bearing stone coal were shown in Table 2. Table 2 suggested that the ash content of the stone coal was 80.54 wt.%, and the content of fixed carbon was very low. The calorific value (2470 kJ/kg) of the vanadium-bearing stone coal was far lower than that of standard coal (29306 kJ/kg), which was not suitable to be used as the raw material of energy.

**Table 1** Chemical composition of raw ore (wt.%)

| $SiO_2$ | $Na_2O$ | $V_2O_5$ | $P_2O_5$ | S | $Al_2O_3$ | CaO |
|---|---|---|---|---|---|---|
| 63.7 | 0.87 | 0.98 | 0.57 | 0.44 | 10.46 | 3.45 |
| TFe | $K_2O$ | $TiO_2$ | MgO | C | Ignition loss | |
| 3.00 | 2.19 | 0.74 | 1.19 | 14.15 | 18.40 | |

**Table 2** Coal industrial analysis results of raw ore

| Parameter | Value |
|---|---|
| Water content/wt.% | 2.01 |
| Calorific value/(kJ·kg$^{-1}$) | 2470 |
| Ash content/wt.% | 80.54 |
| Volatile matter/wt.% | 17.45 |
| Fixed carbon/wt.% | <0.01 |

The X-ray diffraction (XRD) pattern of raw ore was given in Fig. 1. Numerous of characteristic diffraction peaks of quartz were presented in the spectrum. The diffraction peaks of muscovite were covered by quartz, and the diffraction peaks of calcite and goethite could also be observed.

As listed in Table 3, the phase and occurrence of vanadium in raw ore suggested that the vanadium in stone coal mainly existed in the roscoelite (69.90%), followed by tourmaline and

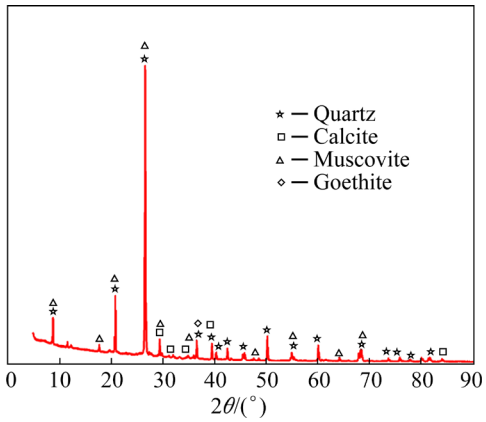


**Fig. 1** XRD pattern of vanadium-bearing stone coal

garnet (16.50%). The rest occurred in limonite and clay minerals, with a distribution rate of 13.59%. A small amount of vanadium existed in vanadium titanium ore as an independent mineral. Besides, there was no vanadium in quartz, potash feldspar, rutile, and barite. The entrainment of vanadium-bearing minerals was shown in Fig. 2.

**Table 3** Phase analysis results of vanadium-bearing stone coal

| Total phase | Content/wt.% | Distribution rate/% |
|---|---|---|
| Vanadium in limonite and clay minerals | 0.14 | 13.59 |
| Vanadium in mica | 0.72 | 69.90 |
| Vanadium in tourmaline and garnet | 0.17 | 16.50 |
| Total | 1.03 | 100 |

The grade and distribution rate of vanadium in each particle size were obtained through screening

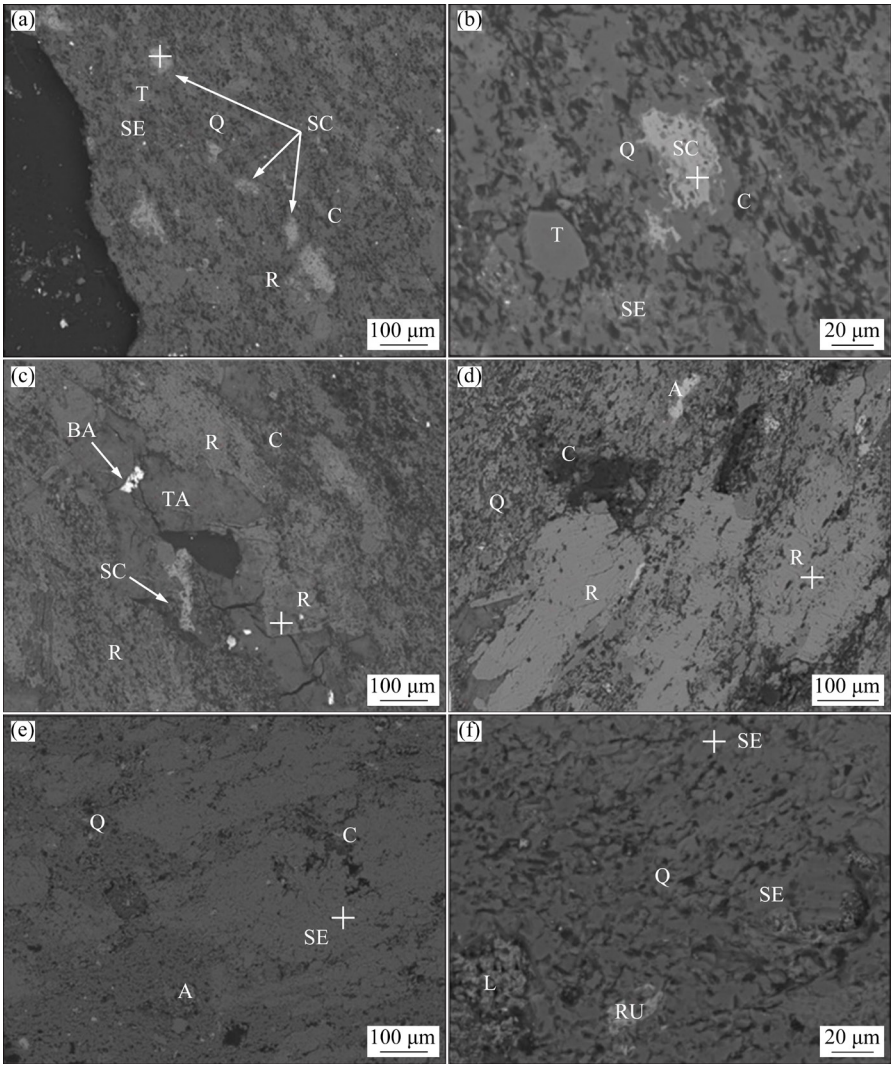


**Fig. 2** Entrainment of vanadium-bearing minerals (SC−Schreyerite; T−Tourmaline; Q−Quartz; SE−Sericite; R−Roscoelite; C−Carbonaceous; BA−Barite; TA−Talcum; A−Apatite; L−Limonite; RU−Rutile): (a, b) Dissemination characteristics of schreyerite; (c, d) Dissemination characteristics of roscoelite; (e, f) Dissemination characteristics of vanadium containing sericite

and chemical analysis, as shown in Table 4. The proportion of <0.074 mm in raw ore accounted for 29.86%, and the vanadium grade was higher in the fine grain.

**Table 4** Particle distribution and vanadium distribution rate in each size fraction of raw ore

| Size fraction/mm | Yield/% | Grade of vanadium/% | Distribution rate of vanadium/% |
|---|---|---|---|
| <0.5 | 16.41 | 0.462 | 15.28 |
| 0.28−0.5 | 19.81 | 0.477 | 12.64 |
| 0.18−0.28 | 7.82 | 0.483 | 7.62 |
| 0.154−0.18 | 10.21 | 0.489 | 10.07 |
| 0.125−0.154 | 4.56 | 0.490 | 4.51 |
| 0.1−0.125 | 4.56 | 0.491 | 4.51 |
| 0.09−0.1 | 3.81 | 0.495 | 3.80 |
| 0.074−0.09 | 2.96 | 0.499 | 2.98 |
| <0.074 | 29.86 | 0.535 | 32.21 |

## 2.2 Experiment procedure

The suspension magnetization roasting system for vanadium-bearing stone coals was illustrated in Fig. 3. 20 g of vanadium-bearing stone coal was placed into a suspension roasting furnace and subjected to single-factor experiments for optimum roasting temperature, time, atmosphere, and gas flow rate. After roasting, the products were cooled to room temperature and analyzed for carbon and vanadium contents.

10 g of roasting products placed in a 100 mL beaker were prepared for leaching experiments in the constant temperature magnetic stirring water bath at sulfuric acid content of 35 wt.%, the liquid/solid ratio of 1.25:1, leaching time of 3 h, and temperature of 90 °C. The leaching products were filtered and dried to detect the content of vanadium. In this study, the leaching rate of vanadium was calculated based on the content of vanadium in leaching residue, as shown in Eq. (1):

$$\eta=\left(1-\frac{m_1\alpha_1}{m_2\alpha_2}\right)\times 100\% \quad (1)$$

where $\eta$ was the leaching rate of vanadium (%); $m_1$ was the mass of leaching residue (g); $m_2$ was the mass of the roasted product (g); $\alpha_1$ was the mass fraction of vanadium in leaching residue (%); $\alpha_2$ was the mass fraction of vanadium in the roasted product (%).

## 2.3 Analysis method

### 2.3.1 X-ray diffraction analysis

X-ray diffraction analysis was mainly used for phase analysis. In this work, the phase transitions of roasted products were investigated by the X-ray diffractometer (Smartlab, Rigaku, Japan). The instrument parameters were as follows: Cu target radiation, Ni filter, pipe voltage 45 kV, pipe current 200 mA, scanning range $2\theta$=5°−90°, step scanning length 0.033°, incoming ray wavelength 1.541 Å, scanning speed 12 (°)/min, and working temperature 25 °C.

### 2.3.2 Scanning electron microscope analysis

The scanning electron microscope (SEM) (ULTRA PLUS, Zeiss, Germany) was adopted to investigate the microstructural evolution of the

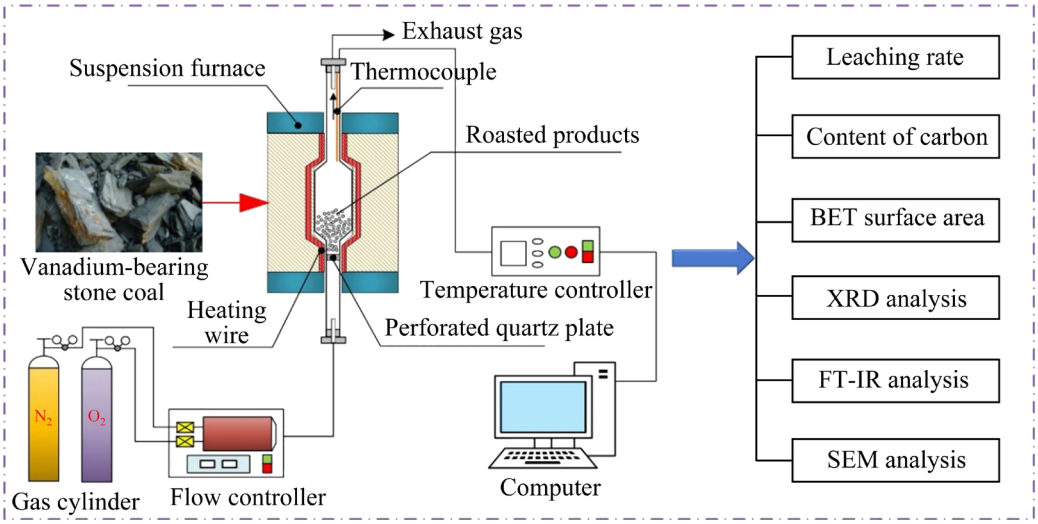


**Fig. 3** Suspension magnetization roasting system for vanadium-bearing stone coals

vanadium-bearing stone coal during the suspension roasting. Mineral particles were embedded and fixed with epoxy resin, then ground and polished, and the sample surface was coated with a 10 nm thick metal (Au) film. The micromorphology of vanadium-bearing stone coal during suspension roasting was obtained at an acceleration voltage of 15 kV.

2.3.3 Fourier transform infrared spectrum analysis

The infrared spectra of vanadium-bearing stone coal during the suspension roasting were ascertained through 380 Fourier transform infrared spectrum (FT-IR) spectrometer (Thermo, USA). The infrared spectra of roasted products were obtained at a scanning resolution of 4 $cm^{-1}$ and the scanning times 128.

2.3.4 Brunauer–Emmett–Teller analysis

Typically, the pores characteristics of solid materials were studied by the Brunauer–Emmett–Teller (BET) analysis with the adsorbent of high purity $N_2$. In this work, the BET surface area analysis of the vanadium-bearing stone coal during the suspension roasting was conducted under $N_2$ adsorption (ASAP 2460, USA).

## 3 Results and discussion

### 3.1 Effect of roasting factors on extraction of vanadium

3.1.1 Roasting temperature

Roasting temperature is the critical factor restricting the roasting effect [30−33]. The carbon in the stone coal cannot be entirely removed, and the mica lattices are difficult to rupture at low temperatures [34]. As the released trivalent vanadium ions cannot be completely oxidized to generate vanadate soluble in acid or water, a low leaching rate of vanadium will be obtained. High temperatures cause the ore to assume a molten state, covering the mineral surface and wrapping valuable vanadium ions to reduce the leaching rate of vanadium. Therefore, the appropriate roasting temperature will allow for maximum vanadium conversion in the roasted product without the appearance of a “glass cover”.

The roasting temperature experiments were conducted in the air atmosphere, with a gas flow rate of 500 mL/min, roasting time of 20 min, and roasting temperatures of 600, 650, 700, 750, 800, and 850 °C, respectively. The contents of carbon and vanadium in the roasted product were detected, and the leaching rates were calculated through the leaching experiments of roasted products, as shown in Fig. 4.

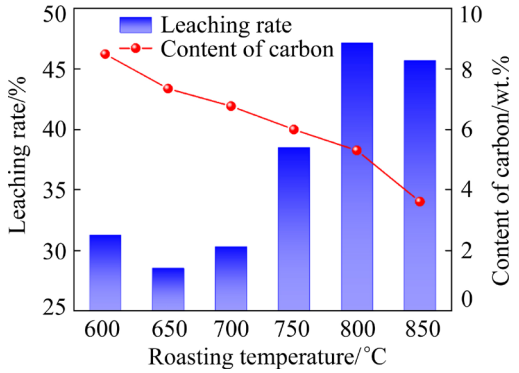


**Fig. 4** Effect of roasting temperature on extraction of vanadium

Figure 4 indicated that the leaching rate of vanadium in stone coal gradually increased with the increase in roasting temperature. The leaching rate remained stable when the temperature was lower than 700 °C. The leaching rate peaked at 47.18% at a roasting temperature of 800 °C. The leaching rate declined to 45.74% at a roasting temperature of 850 °C. It was concluded that the mica lattices were destroyed and several low valence vanadates were oxidized to enhance the leaching of vanadium in stone coal at appropriately high temperatures. However, the molten material would be generated at a higher temperature to restrain the leaching of vanadium. In addition, the contents of carbon in roasted products gradually decreased with the increase in roasting temperature, which suggested that the violent decarburization reaction occurred at the roasting temperature over 800 °C. Since the carbon was a reducing substance, which would restrain the transformation of vanadium in the process of oxidation roasting, the reduction of carbon also promoted the leaching rate of vanadium. Therefore, the optimum roasting temperature was considered to be 800 °C.

3.1.2 Roasting time

Roasting time determines the progress of the chemical reaction. The stone coal was fully oxidized, and the phase transformation process was promoted by appropriate roasting time. Meanwhile, the reducing substances in stone coal, such as carbon, would be removed more fully. However, due to the relatively low carbon and vanadium

contents in stone coal, the vanadium extraction effect would not be improved by prolonging the roasting time at the critical time of complete oxidation, and the additional energy was wasted.

Experiments were performed on the roasting time conditions of stone coal at a roasting temperature of 800 °C, a gas flow rate of 500 mL/min, and roasting time of 5, 10, 15, 20, and 25 min, respectively. The contents of carbon and vanadium in the roasted product were detected, and the leaching rates were calculated through the leaching experiments of roasted products, as shown in Fig. 5.

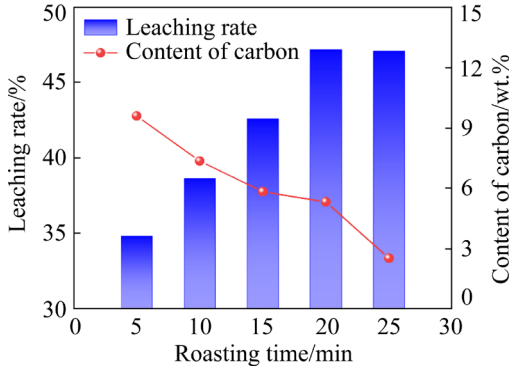


**Fig. 5** Effect of roasting time on extraction of vanadium

From Fig. 5, with the increase in roasting time, the leaching rate of vanadium increased gradually. When the roasting time was 20 min, the leaching rate of vanadium reached 47.18%, and the leaching rate of vanadium was 47.09% at the roasting time of 25 min. Hence, the appropriate roasting time was 20 min. This phenomenon suggested that the oxidation conversion of vanadium stone coal could be effectively improved by prolonging the roasting time at the same temperature. Meanwhile, the roasting time determined the conversion of vanadium. When the free vanadium in the stone coal was completely oxidized at enough roasting time, the roasting temperature regulated the vanadium leaching rate. Besides, the carbon content decreased from 12.80 wt.% to 2.51 wt.% during the roasting process. Reducing materials would restrain the oxidation of vanadium. Thus, decarbonization was very important to improve the roasting effect.

3.1.3 Gas flow rate

The gas flow rate affects the fluidization state of the material in the roaster, thus regulating the reaction rate and leaching rate. For the roasting experiments, the effects of different gas flow rates on the results were investigated at a roasting temperature of 800 °C, a roasting time of 20 min, and gas flow rates of 100, 200, 300, 400, and 500 mL/min, respectively. The contents of carbon and leaching rates at different gas flow rates are shown in Fig. 6.

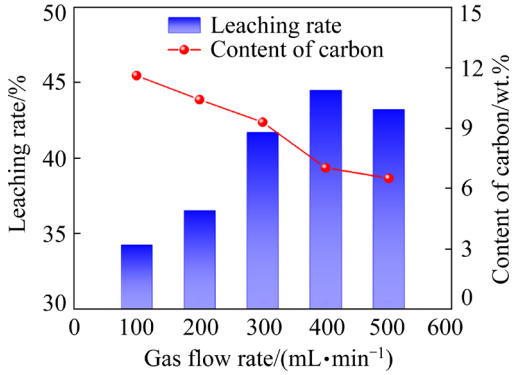


**Fig. 6** Effect of gas flow rate on extraction of vanadium

Figure 6 suggested that with the increase of gas flow rate into the calciner, the leaching rate of vanadium in stone coal increased gradually and then tended to be stable. The leaching rate increased from 34.28% to 44.51% as the gas flow rate varied from 100 to 400 mL/min. The leaching rate of vanadium was 43.23% at the gas flow of 500 mL/min. The carbon content in stone coal gradually decreased with the increase in gas flow rate, and decreased to 6.5 wt.% at the gas flow rate of 500 mL/min. Therefore, the optimum gas flow rate was 400 mL/min.

### 3.2 Effect of roasting factors on phase transition

3.2.1 Roasting temperature

X-ray diffraction analysis was undertaken on the roasted products at 600, 650, 700, 750, 800, and 850 °C, as shown in Fig. 7. Diffraction peaks of hematite appeared in the roasted sample at 600 °C. Meanwhile, the intensity gradually increased with increasing temperature, pointing to the slow decomposition of goethite into hematite in the raw ore. During the roasting process of illite, interlayer water and adsorbed water would be removed first. Due to eliminating hydroxyl groups from illite, dehydrated illite will be produced as the temperature increases. The dehydrated illite still retained the layered framework structure of illite. As the temperature reaches 1100 °C, the layered crystal structure of dehydrated illite will be destroyed to form an amorphous phase. The

diffraction peaks of sericite gradually were weakened with increased roasting temperature, illustrating that its construction began to be destroyed, and some vanadium present in mica lattice was released [35,36], authenticating the rapid increase in the leaching rate of vanadium at temperatures higher than 700 °C. Besides, the diffraction characteristic peak of calcite gradually decreased with the increase in roasting temperature. Finally, it disappeared at approximately 800 °C, indicating that the calcite in the raw ore was wholly decomposed. The structures of quartz and muscovite were destroyed with the increase in roasting temperature. The diffraction peaks of orthoclase also appeared in the roasted products. The intensity of the peaks firstly increased and then decreased with the temperature rise, indicating that the reaction between quartz and mica occurred at low temperature to generate the orthoclase phase. Orthoclase minerals continued to react with mica at high temperatures.

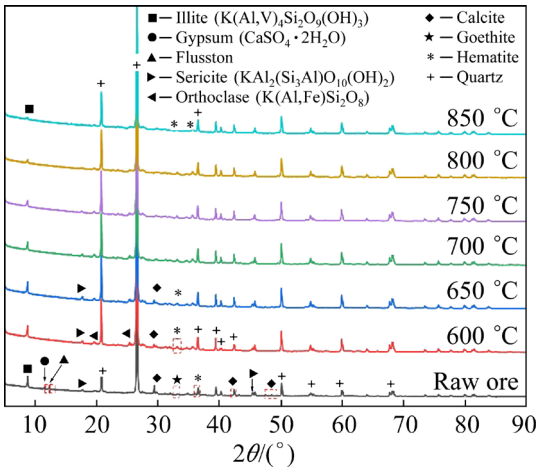


**Fig. 7** XRD patterns of roasted products at different temperatures

3.2.2 Roasting time

An X-ray diffraction analysis of the roasted products at roasting time from 5 to 25 min was performed to investigate the effect of roasting time on the phase transformation of stone coal, as depicted in Fig. 8. Figure 8 suggested that the diffraction peaks of calcite and anhydrite disappeared after roasting, and the goethite was transformed into hematite. With the increase in roasting time, the characteristic diffraction peak intensity of illite and sericite dropped noticeably, pointing to the removal of the hydroxyl group of illite and the destruction of the layered structure of sericite [35,36], which is a fundamental explanation for the observed gradual increase in the leaching rate. The intensity of diffraction peak of sericite at a roasting time of 25 min was close to that at a roasting time of 20 min. The destruction of mica lattice mainly depended on the roasting temperature, consistent with the experimental results.

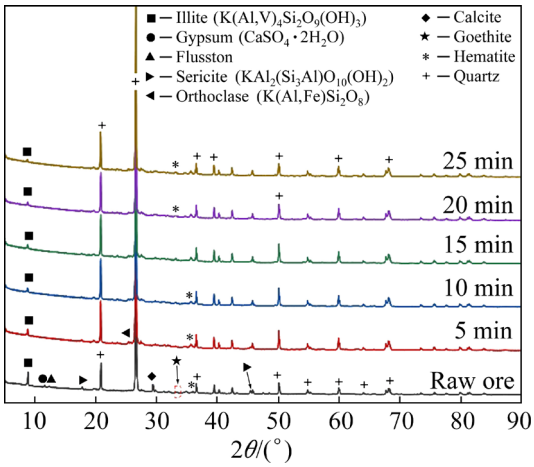


**Fig. 8** XRD patterns of roasted products at different roasting time

3.2.3 Gas flow rate

The X-ray diffraction analysis results of roasted products at gas flow rates of 100, 200, 300, 400, and 500 mL/min were exhibited in Fig. 9 to explore the effects of gas flow rate on the phase transformation of stone coal during the roasting process. From Fig. 9, owing to the removal of hydroxyl groups from illite, the intensity of the diffraction characteristic peak of illite decreased gradually with the increase in the gas flow rate. The characteristic peaks of gypsum also disappeared after roasting, and no new diffraction peaks appeared. With the rise of gas flow rate, the intensity of the diffraction peak of sericite gradually was weakened and reached the minimum at the gas flow rate of 400 mL/min. There was a slight variation in the intensity of the diffraction peak of sericite as the gas flow rate increased to 500 mL/min, which was consistent with the experiment results of leaching rate.

Moreover, the diffraction peak of orthoclase appeared in the roasted samples, and the intensity of the diffraction peak of quartz was weakened after roasting [35,36]. It was concluded that quartz was participated to form feldspar substances in the roasting process. The diffraction peak of calcite

completely disappeared after roasting, and the goethite was also completely decomposed into hematite.

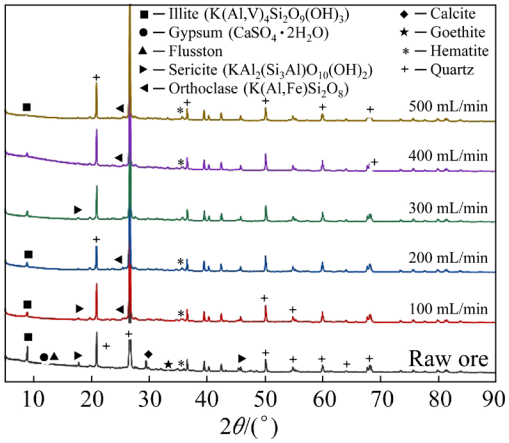


**Fig. 9** XRD patterns of roasted products at different gas flow rates

### 3.3 Structural variation of stone coal during suspension roasting

The Fourier transform infrared spectra of the roasted products at different roasting temperatures in the wavenumber range of 400−4000 $cm^{-1}$ are given in Fig. 10. The absorption peaks of 3693 and 3619 $cm^{-1}$ belonged to the stretching vibration absorption peaks of the outer hydroxyl group and the inner hydroxyl group of the vanadium-bearing mica [35,36], respectively. Two absorption peaks disappeared at 600 °C, and the internal and external hydroxyl groups of mica were removed entirely. The absorption peak of calcite at 1424 $cm^{-1}$ disappeared utterly when the roasting temperature exceeded 800 °C, indicating that the calcite structure in the raw ore was destroyed entirely [35,36]. Meanwhile, CaO produced by the decomposition reaction could promote the transformation of vanadate, thus improving the leaching rate of vanadium. The absorption bands at about 1081 and 1032 $cm^{-1}$ represented the stretching vibration peaks of Si—O. The absorption peak at about 1032 $cm^{-1}$ disappeared at a roasting temperature of 600 °C, which suggested that the Si—O bond fractured and the structure of mica bearing vanadium began to be destroyed.

FT-IR analysis of roasted products with different roasting time for discussing the effect of roasting time on the phase change of stone coal was undertaken, and the results are shown in Fig. 11. The stretching vibration absorption peaks of the outer and inner hydroxyl groups of the mica containing vanadium disappeared completely at a roasting time of 5 min, indicating that the inner and outer hydroxyl groups of the mica containing vanadium were destroyed. The absorption peaks of 3693 and 3619 $cm^{-1}$ would be unchanged with the increase in roasting time, which indicated that the hydroxyl water of vanadium-bearing mica in stone coal raw ore was wholly removed. The absorption peak at 1424 $cm^{-1}$ was unique to calcite, which was generated by stretching vibration and bending vibration of the $CO_3^{2-}$ group. As the roasting time reached 5 min, the absorption peak of calcite disappeared utterly, which suggested that the calcite in stone coal would decompose rapidly at the roasting temperature of 800 °C. The high-strength

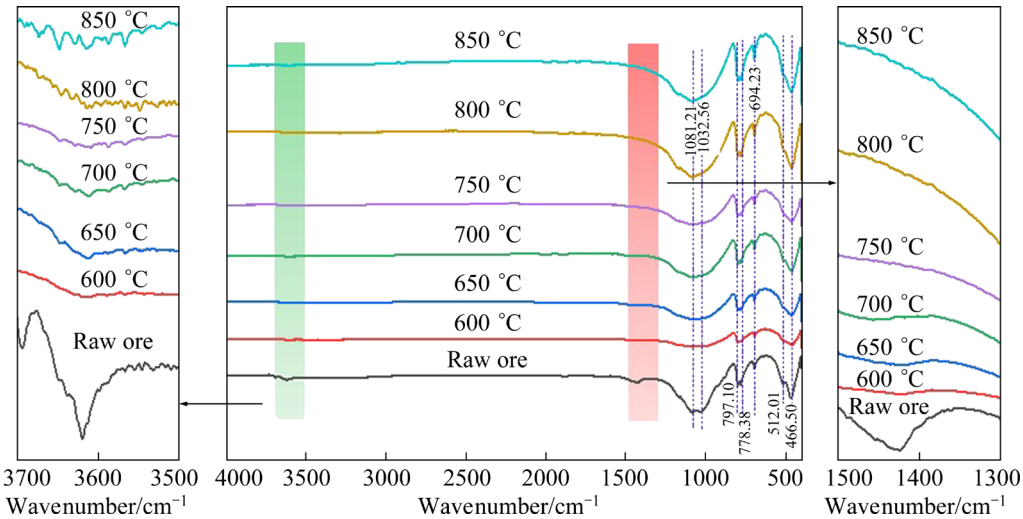


**Fig. 10** FT-IR spectra of roasted products at different roasting temperatures

absorption bands at about 1081 and 1032 $cm^{-1}$ were the stretching vibration peaks of Si—O, and the absorption peak at about 1032 $cm^{-1}$ disappeared with the increase in roasting time, which indicated that the Si—O bond fractured and the structure of vanadium-bearing mica began to be destroyed [35,36].

### 3.4 Morphology evolution of stone coal during suspension roasting

The microstructures of the stone coal raw ore and the roasted products at 600, 800 and 850 °C can be observed in the SEM images, as illustrated in Fig. 12. Figure 12(a) showed that the morphology of mineral particles presented a large number of irregular lamellar aggregates covering the surface of mineral particles. The side of the particles gave an apparent layered stacking shape, which belonged to layered silicate minerals. From Fig. 12(b), after being roasted at 600 °C, more irregular small particles appeared on the surface, although the roasted mineral particles retained the layered structure. The layered structure of silicate minerals was slightly damaged to produce cracks. Many small particles appeared with a rougher structure in

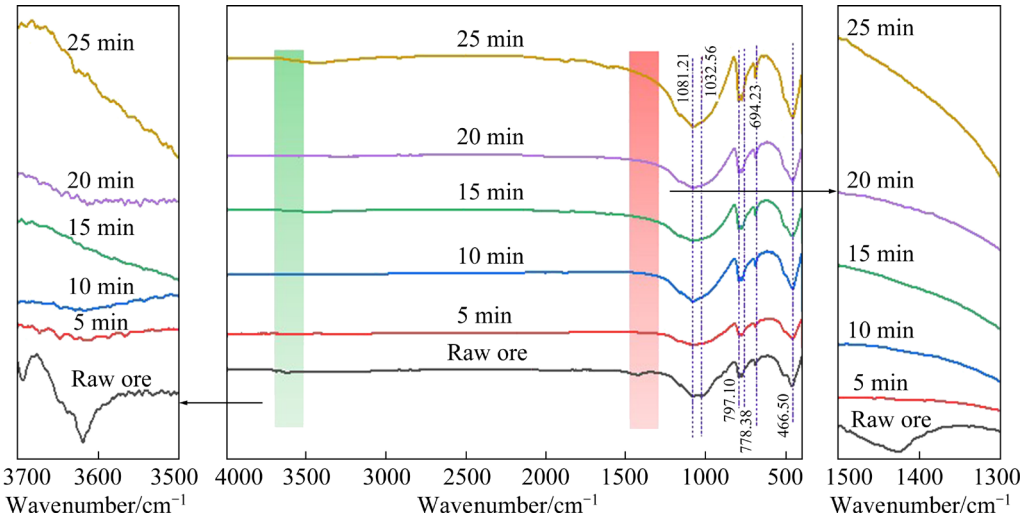


**Fig. 11** FT-IR spectra of roasted products at different roasting time

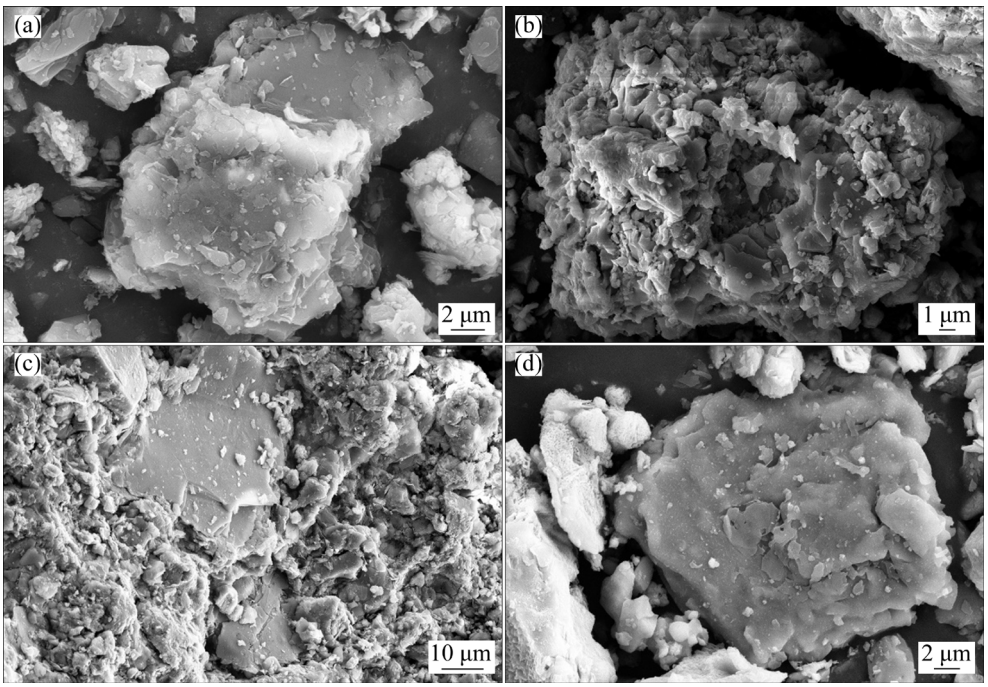


**Fig. 12** SEM images of raw ore and roasted samples at different roasting temperatures: (a) Raw ore; (b) 600 °C; (c) 800 °C; (d) 850 °C

the micromorphology of roasted products at 800 °C (Fig. 12(c)). The irregular fracture surface was generated, and the layered structure was further destroyed.

Meanwhile, the surface of roasted products became loose and porous, which was more conducive to the reaction between gas and solid, thus improving the solid−liquid response in subsequent leaching. Figure 12(d) indicated that the sintering phenomenon of the stone coal appeared at a roasting temperature of 850 °C. The rough surface of mineral particles disappeared, and the tiny particles decreased suddenly. Instead, the surface of roasted products became smooth due to the particles bonded by the liquid phase, and a large number of pores were filled by the liquid phase, which reduced the specific surface area. The compact structure reduced the effect of oxidation roasting and seriously inhibited the leaching of vanadium, resulting in the poor impact of vanadium extraction. All in all, with the increase in roasting temperature, the surface of mineral particles gradually became rough and irregular. A large number of fine particles were produced, and the specific surface area of materials gradually increased, which was conducive to the oxidation of stone coal and the leaching of vanadium. However, a severe sintering phenomenon was generated on the surface of roasted products as the temperature was over 850 °C. The liquid phase covered the surface of roasted products to decrease the leaching rate.

### 3.5 Pore distribution characteristics of stone coal during suspension roasting

The $N_2$ adsorption−desorption isotherm curves and pore size distribution of the raw ore and roasted products at 600, 800 and 850 °C are shown in Figs. 13 and 14, respectively. The pore parameters of samples are tabulated in Table 5.

Figure 13(b) suggested that after the samples were roasted at 600 °C, the adsorption and desorption branches coincided at relative pressure $P/P_0$<0.4. The adsorption capacity increased slowly with the increase in relative pressure. The adsorption capacity increased sharply as the relative pressure was close to 1. The desorption curve began

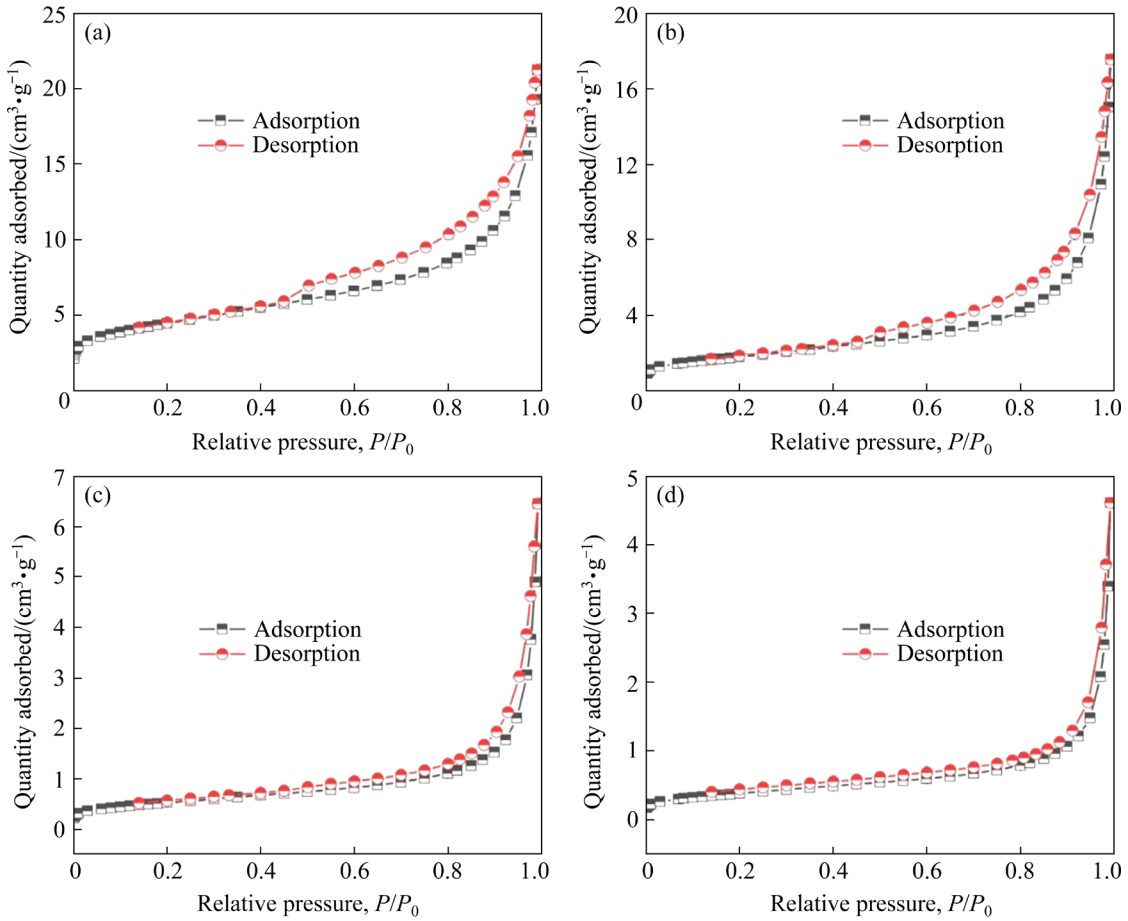


**Fig. 13** Adsorption−desorption isotherm curves of raw ore and roasted samples at different temperatures: (a) Raw ore; (b) 600 °C; (c) 800 °C; (d) 850 °C

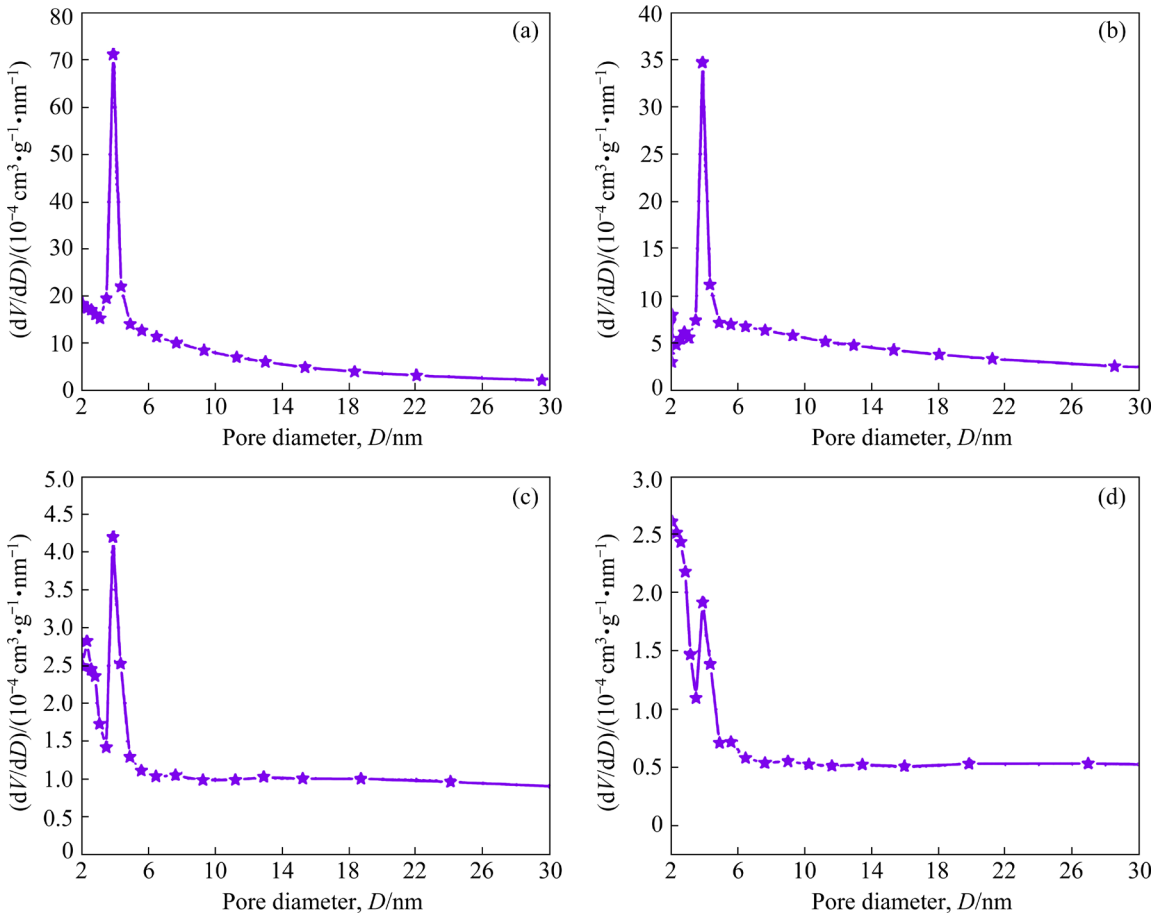


**Fig. 14** Pore diameter distribution of raw ore and roasted samples at different temperatures: (a) Raw ore; (b) 600 °C; (c) 800 °C; (d) 850 °C

**Table 5** Pore parameters of stone coal raw ore and roasted products at different temperatures

| Sample | Specific surface area/($m^2 \cdot g^{-1}$) | Total pore volume/($cm^3 \cdot g^{-1}$) | Average pore size/nm |
|---|---|---|---|
| Raw ore | 15.63 | 0.022 | 5.28 |
| 600 °C | 6.45 | 0.013 | 8.06 |
| 800 °C | 1.90 | 0.003 | 7.35 |
| 850 °C | 1.39 | 0.002 | 6.67 |

to separate from the adsorption curve at $P/P_0$<1, and gradually overlapped with the adsorption curve at $P/P_0$=0.5, which was considered as the typical H3 adsorption loop. The adsorption−desorption isotherm curve of roasted products at 800 °C (Fig. 13(c)) suggested that the adsorption capacity increased slowly with the increase in relative pressure at $P/P_0$<0.8, which expanded rapidly at $P/P_0$>0.9. The desorption and adsorption curves generated a narrow atypical adsorption loop, which belonged to the superposition of H3 and H4 loops. Compared with the adsorption−desorption isotherm curves of roasted products at 600 and 800 °C, the closed-loop of adsorption in the curve roasted at 850 °C (Fig. 13(d)) continued to decrease and nearly disappeared.

Figure 14 suggested that the pores volume in roasted products of 600 °C was nearly half that of the raw stone coal, with the most probable pore size of 4 nm, which indicated that the number of pores decreased. Yet, the distribution of pores was consistent with the raw stone coal. The pores volume of 800 °C roasted products was reduced from 0.013 to 0.003 $cm^3/g$ compared with the roasted sample at 600 °C, and the most probable pore size was still approximately 4 nm. Mesopores still dominated the roasted product of 800 °C, and there were fewer small holes and macropores. The total pore volume of roasted products at 850 °C was 0.002 $cm^3/g$, and the most probable pore size was about 2 nm.

In conclusion, the specific surface area and the number of pores decreased sharply with the increase in roasting temperature, but the distribution

of pores had a slight change. The pore structure gradually transformed from an open pore at both ends to a closed pore at one end.

### 3.6 Phase reconstruction and vanadium transformation behavior during suspension roasting

The vanadium in raw ore was mainly distributed in muscovite and vanadium titanium ore. The chemical formula of vanadium-bearing muscovite was $K(Al,V)_2[AlSi_3O_{10}](OH)_2$. The vanadium titanate was the independent mineral of vanadium and titanium in ore, and the chemical formula was $V_2Ti_3O_9$. Na mainly existed in albite ($NaAlSi_3O_8$), while Ca primarily existed in the form of calcite ($CaCO_3$).

Since the content of $SiO_2$ in stone coal was high, the diffraction peaks of trace substances were not evident during the X-ray diffraction analysis of samples. Given this phenomenon, the XRD pattern was processed in several stages. The diffraction peak of quartz with the most considerable intensity was removed to observe the phase transformation in the roasting process, as shown in Fig. 15.

The vanadium in the mica was released from the vanadium oxygen octahedron and oxidized to V(V) or V(IV) under oxygen and high temperature. The vanadium mica existed in dehydroxylated mica after losing hydroxyl and vanadium, with low crystallinity and poor stability [37,38]. The chemical reactions that occurred during this period were as follows:

$$K(Al,V)_2[AlSi_3O_{10}](OH)_2+2O_2=V_2O_5+KAl_2[AlSi_3O_{10}]+H_2O \quad (2)$$

V(III) in vanadium titanium ore would be oxidized to V(IV) under the action of oxygen. Following this, Ti(IV) in vanadium titanium ore lattice was promptly replaced by V(IV), and V(IV) would be further oxidized to V(V) in oxygen.

$$V_2Ti_3O_9+1/2O_2=VO_2+3TiO_2 \quad (3)$$

$$2VO_2+1/2O_2=V_2O_5 \quad (4)$$

The separated vanadium would exist in vanadate and was dissolved in the leaching process. In addition, during the suspension roasting process,

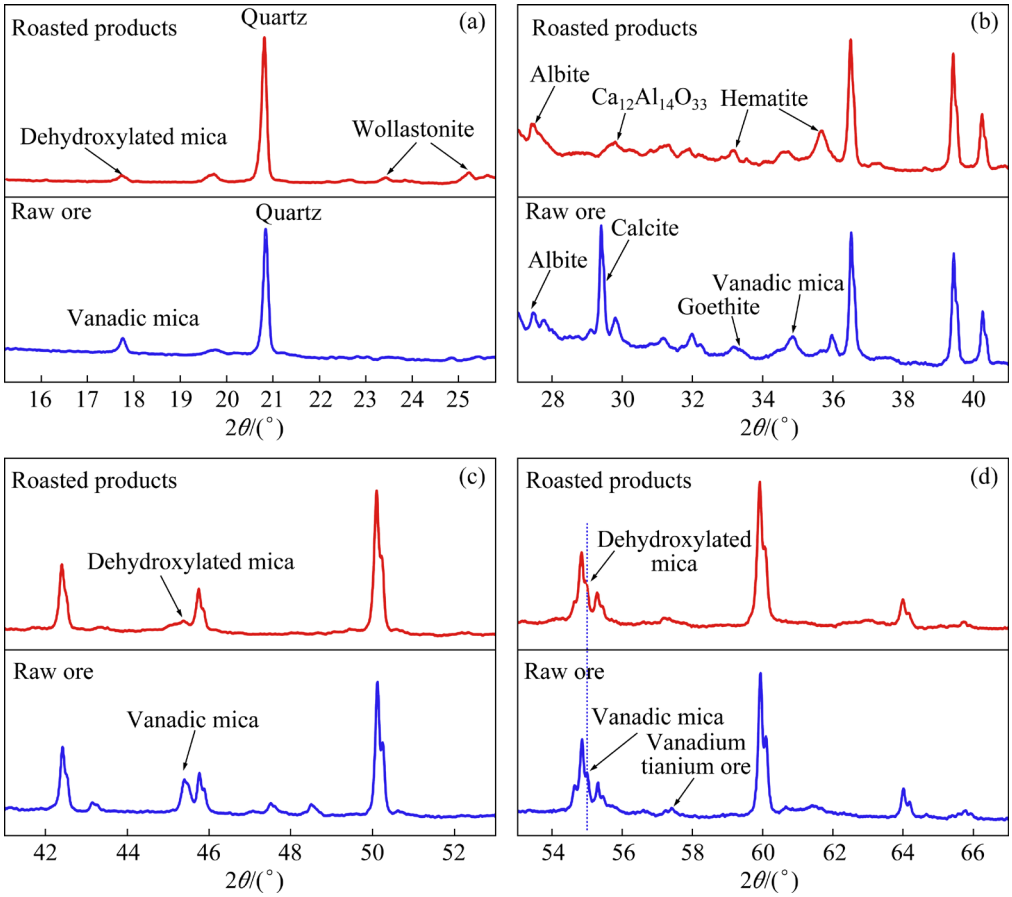


**Fig. 15** XRD patterns of raw ore and roasted product at different $2\theta$ values: (a) 15°−26°; (b) 27°−41°; (c) 41°−53°; (d) 53°−67°

the diffraction peaks of albite were almost the same as those of the raw ore, indicating that the structure of albite was unchanged. New phases containing calcium appeared with the decomposition of calcite [37,38]. The $Ca_{12}Al_{14}O_{33}$ was generated through the reaction between CaO and $Al_2O_3$. Besides, the wollastonite was produced via the reaction of CaO and $SiO_2$. The chemical reactions were as follows:

$$7Al_2O_3+12CaO=Ca_{12}Al_{14}O_{33} \quad (5)$$

$$SiO_2+CaO=CaSiO_3 \quad (6)$$

## 4 Conclusions

(1) An innovative technology of suspension roasting-leaching was proposed to extract vanadium from refractory stone coal. The leaching rate of vanadium was improved from 20% previously to 47.18% in the present technology at a roasting temperature of 800 °C, a roasting time of 20 min, and a gas flow rate of 400 mL/min.

(2) The surface of stone coal gradually became rough and irregular with the increased roasting temperature. Many fine particles were produced, and the specific surface area gradually increased, which was favorable to the occurrence of oxidation reaction and the subsequent leaching process. The lamellar structure of roscoelite was progressively destroyed upon the roasting reaction, and the release and transformation of vanadium were relatively thorough. Consequently, the leaching rate of vanadium was improved via suspension roasting.

(3) The vanadium was released and oxidized to V(V) or V(IV) via the suspension roasting. In parallel, the roscoelite existed in dehydroxylated mica after losing hydroxyl and vanadium. The separated vanadium existed in vanadate, and then was dissolved in the leaching process. In addition, since the CaO was formed during the roasting process, $Ca_{12}Al_{14}O_3$ and wollastonite were generated through the reactions of CaO, $Al_2O_3$, and $SiO_2$.

## Acknowledgments

This research work was supported by the Fundamental Research Funds for the Central Universities (No. N2101023), the National Key Research and Development Program of China (No. 2018YFC1901901902), the National Natural Science Foundation of China (Nos. 51904058, 52104247, 52130406), and the Open Foundation of State Key Laboratory of Mineral Processing, China (No. BGRIMM-KJSKL-2020-17), for which the authors express their appreciation.

## References

[1] MOSKALYK R R, ALFANTAZI A M. Processing of vanadium: A review [J]. Minerals Engineering, 2003, 16(9): 793−805.

[2] ZHANG Yi-min, BAO Shen-xu, LIU Tao, CHEN Tie-jun, HUANG Jing. The technology of extracting vanadium from stone coal in China: History, current status and future prospects [J]. Hydrometallurgy, 2011, 109(1/2): 116−124.

[3] ZHAO Long-sheng, WANG Li-na, QI Tao, CHEN De-sheng, ZHAO Hong-xin, LIU Ya-hui. A novel method to extract iron, titanium, vanadium, and chromium from high-chromium vanadium-bearing titanomagnetite concentrates [J]. Hydrometallurgy, 2014, 149: 106−109.

[4] PERRY M L. Expanding the chemical space for redox flow batteries [J]. Science, 2015, 349(6255): 1452−1452.

[5] ZENG Yi-kai, ZHAO Tian-shou, AN Liang, ZHOU Xue-long, WEI Lei. A comparative study of all-vanadium and iron−chromium redox flow batteries for large-scale energy storage [J]. Journal of Power Sources, 2015, 300: 438−443.

[6] DAI Shi-feng, ZHENG Xue, WANG Xi-bo, FINKELMAN R B, JIANG Yao-fa, REN De-yi, YAN Xiao-yun, ZHOU Yi-ping. Stone coal in China: A review [J]. International Geology Review, 2018, 60(5/6): 736−753.

[7] HU Yang-jia, ZHANG Yi-ming, BAO Shen-xu, LIU Tao. Effects of the mineral phase and valence of vanadium on vanadium extraction from stone coal [J]. International Journal of Minerals, Metallurgy, and Materials, 2012, 19(10): 893−898.

[8] WANG Ming-yu, XIAO Lian-sheng, LI Qing-gang, WANG Xue-wen, XIANG Xiao-yan. Leaching of vanadium from stone coal with sulfuric acid [J]. Rare Metals, 2009, 28(1): 1−4.

[9] LIU Xin, ZHANG Yi-min, LIU Tao, CAI Zhen-lei, SUN Kun. Pre-concentration of vanadium from stone coal by gravity using fine mineral spiral [J]. Minerals, 2016, 6(3): 82.

[10] ZHAO Yun-liang, ZHANG Yi-min, LIU Tao, CHEN Tie-jun, BIAN Ying, BAO Shen-xu. Pre-concentration of vanadium from stone coal by gravity separation [J]. International Journal of Mineral Processing, 2013, 121: 1−5.

[11] WANG Li, SUN Wei, ZHANG Qing-peng. Recovery of vanadium and carbon from low-grade stone coal by flotation [J]. Transactions of Nonferrous Metals Society of China, 2015, 25(11): 3767−3773.

[12] WANG Li, SUN Wei, LIU Run-qing, GU Xiao-chuan.

Flotation recovery of vanadium from low-grade stone coal [J]. Transactions of Nonferrous Metals Society of China, 2014, 24(4): 1145−1151.

[13] LIU Chun, ZHANG Yi-min. BAO Shen-xu. Vanadium recovery from stone coal through roasting and flotation [J]. Transactions of Nonferrous Metals Society of China, 2017, 27(1): 197−203.

[14] LI Min-ting, WEI Chang, FAN Gand, LI Cun-xiong, DENG Zhi-gan, LI Xin-bin. Extraction of vanadium from black shale using pressure acid leaching [J]. Hydrometallurgy, 2009, 98(3/4): 308−313.

[15] ZHU Yang-ge, ZHANG Guo-fan, FENG Qi-ming, LU Yi-ping, OU Le-ming, HUANG Si-jie. Acid leaching of vanadium from roasted residue of stone coal [J]. Transactions of Nonferrous Metals Society of China, 2010, 20(S): s107−s111.

[16] LI Hong-yi, WANG Kang, HUA Wei-hao, YANG Zhao, ZHOU Wang, XIE Bing. Selective leaching of vanadium in calcification-roasted vanadium slag by ammonium carbonate [J]. Hydrometallurgy, 2016, 160: 18−25.

[17] WANG Tai-ying, XU Long-jun, LIU Chen-lun, ZHANG Zhao-di. Calcified roasting−acid leaching process of vanadium from low-grade vanadium-containing stone coal [J]. Chinese Journal of Geochemistry, 2014, 33(2): 163−167.

[18] YAN Bai-jun, WANG Da-ya, WU Liu-shun, DONG Yuan-chi. A novel approach for pre-concentrating vanadium from stone coal ore [J]. Minerals Engineering, 2018, 125: 231−238.

[19] WANG Fei, ZHANG Yi-min, LIU Tao, HUANG Jing, ZHAO Jie, ZHANG Guo-bin, LIU Juan. Comparison of direct acid leaching process and blank roasting acid leaching process in extracting vanadium from stone coal [J]. International Journal of Mineral Processing, 2014, 128: 40−47.

[20] CAI Zhei-lei, ZHANG Yi-min, LIU Tao, HUANG Jing. Vanadium extraction from refractory stone coal using novel composite additive [J]. Journal of Metals, 2015, 67(11): 2629−2634.

[21] LI Xin-sheng, XIE Bing. Extraction of vanadium from high calcium vanadium slag using direct roasting and soda leaching [J]. International Journal of Minerals, Metallurgy, and Materials, 2012, 19(7): 595−601.

[22] LIU Yan-hua, YANG Chao, LI Pei-you, LI Shi-qi. A new process of extracting vanadium from stone coal [J]. International Journal of Minerals, Metallurgy, and Materials, 2010, 17(4): 381−388.

[23] ZENG Xi, WANG Fang, ZHANG Hui-feng, CUI Li-jie, YU Jian, XU Guang-wen. Extraction of vanadium from stone coal by roasting in a fluidized bed reactor [J]. Fuel, 2015, 142: 180−188.

[24] DU Guang-chao, FAN Chuan-lin, YANG Hai-tao, ZHU Qing-shan. Selective extraction of vanadium from pre-oxidized vanadium slag by carbochlorination in fluidized bed reactor [J]. Journal of Cleaner Production, 2019, 237: 117765.

[25] TANG Zhi-dong, ZHANG Qi, SUN Yong-sheng, GAO Peng, HAN Yue-xin. Pilot-scale extraction of iron from flotation tailings via suspension magnetization roasting in a mixture of CO and $H_2$ followed by magnetic separation [J]. Resources, Conservation and Recycling, 2021, 172: 105680.

[26] SUN Yong-sheng, ZHU Xin-ran, HAN Yue-xin, LI Yan-jun, GAO Peng. Iron recovery from refractory limonite ore using suspension magnetization roasting: A pilot-scale study [J]. Journal of Cleaner Production, 2020, 261: 121221.

[27] ZHANG Xiao-long, HAN Yue-xin, SUN Yong-sheng, LI Yan-jun. Innovative utilization of refractory iron ore via suspension magnetization roasting: A pilot-scale study [J]. Powder Technology, 2019, 352: 16−24.

[28] YUAN Shuai, XIAO Han-xin, YU Tian-yi, LI Yan-jun, GAO Pao. Enhanced removal of iron minerals from high-iron bauxite with advanced roasting technology for enrichment of aluminum [J]. Powder Technology, 2020, 372: 1−7.

[29] YUAN Shuai, ZHOU Wen-tao, HAN Yue-xin, LI Yan-jun. Efficient enrichment of low-grade refractory rhodochrosite by preconcentration−neutral suspension roasting−magnetic separation process [J]. Powder Technology, 2020, 361: 529−539.

[30] GENG Shu-hua, LI Guang-shi, ZHAO Yong, CHENG Hong-wei, LU Yi, LU Xiong-gang, XU Qian. Extraction of valuable metals from low nickel matte by calcified roasting−acid leaching process [J]. Transactions of Nonferrous Metals Society of China, 2019, 29(10): 2202−2212.

[31] LI Xiao-bin, WANG Hong-yang, ZHOU Qiu-sheng, QI Tian-gui, LIU Gui-hua, PENG Zhi-hong, WANG Yi-lin. Reaction behavior of kaolinite with ferric oxide during reduction roasting [J]. Transactions of Nonferrous Metals Society of China, 2019, 29(1): 186−193.

[32] WANG Hong-jun, FENG Ya-li, LI Hao-ran, KANG Jin-xing. Simultaneous extraction of gold and zinc from refractory carbonaceous gold ore by chlorination roasting process [J]. Transactions of Nonferrous Metals Society of China, 2020, 30(4): 1111−1123.

[33] YUAN Shuai, WANG Ruo-feng, GAO Peng, HAN Yue-xin, LI Yan-jun. Suspension magnetization roasting on waste ferromanganese ore: A semi-industrial test for efficient recycling of value minerals [J]. Powder Technology, 2022, 396: 80−91.

[34] YUAN Yi-zhong, ZHANG Yi-min, HU Peng-cheng. Formation mechanism and control method of the silicate minerals-based coating (SMC) in blank roasting process of vanadium-bearing shale [J]. Colloids and Surface A: Physicochemical and Engineering Aspects, 2020, 592: 124535.

[35] DÖBELIN N, REZNITSKY L Z, SKLYASROV E V, ARMBRUSTER T, MEDENBACH O. Schreyerite, $V_2Ti_3O_9$: New occurrence and crystal structure [J]. American Mineralogist, 2006, 91(1): 196−202.

[36] ZHAO Yun-liang, WANG Wei, ZHANG Yin-min, SONG Shao-xian, BAO Shen-xu. In-situ investigation on mineral

phase transition during roasting of vanadium-bearing stone coal [J]. Advanced Powder Technology, 2017, 28(3): 1103−1107.

[37] ZHANG Cheng-qiang, SUN Chuan-yao, LI Hang, YIN Wan-zhong, ZHOU Jun-jie. Blank roasting kinetics of illite type vanadium bearing stone coal [J]. Journal of Materials Research and Technology, 2020, 9(4): 7363−7369.

[38] ZHANG Yin-min, HU Yang-jia, BAO Shen-xu. Vanadium emission during roasting of vanadium-bearing stone coal in chlorine [J]. Minerals Engineering, 2012, 30: 95−98.

# 悬浮焙烧法强化从难选石煤中提取钒

袁 帅[1,2]，秦永红[1,2]，金永鹏[1,2]，李艳军[1,2]

1. 东北大学 资源与土木工程学院，沈阳 110819；
2. 难采选铁矿资源高效开发利用技术国家地方联合工程研究中心，沈阳 110819

**摘 要**：提出一种难选石煤在空气气氛下悬浮焙烧−酸浸强化的提钒新技术。在焙烧温度为 800 ℃、焙烧时间为 20 min、气体流量为 400 mL/min 的条件下钒的浸出率从过去的 20%提高到目前技术的 47.14%。在焙烧过程中，石煤表面逐渐变得粗糙和不规则，颗粒比表面积增加，硅酸盐矿物的片状结构被破坏，促进了钒的释放。同时，石煤中的钒被氧化为 V(V)或 V(IV)。结果表明，由于悬浮焙烧过程中钒的释放和转化，因此，其浸出率得到了提高。

**关键词**：石煤；钒；悬浮焙烧；浸出；矿相重构；显微组织

**(Edited by Wei-ping CHEN)**